

OMAE2016-54211

A FINITE ELEMENT MODEL OF 18650 LITHIUM-ION BATTERY FOR EXPLOSION CAUSED BY INTERNAL SHORT CIRCUIT

Lubing Wang

¹Department of Automotive Engineering, School of Transportation Science and Engineering, Beihang University, Beijing, China, 100191

²Advanced Vehicle Research Center (AVRC), Beihang University, Beijing, China, 100191

Binghe Liu

¹Department of Automotive Engineering, School of Transportation Science and Engineering, Beihang University, Beijing, China, 100191

²Advanced Vehicle Research Center (AVRC), Beihang University, Beijing, China, 100191

Jun Xu

¹Department of Automotive Engineering, School of Transportation Science and Engineering, Beihang University, Beijing, China, 100191

²Advanced Vehicle Research Center (AVRC), Beihang University, Beijing, China, 100191

³State Key Laboratory of Nonlinear Mechanics (LNM), Institute of Mechanics, Chinese Academy of Sciences, Beijing 100190, China

ABSTRACT

The lithium-ion battery (LIB) is widely used in portable devices, power tools and electric vehicles, which becomes one of the most important moving power sources. However, inevitable internal short circuits may cause the pressure inside the battery rising, leading to fire or intensive explosion. In this paper, a finite element (FE) model is established to reasonably capture the major explosion behavior of 18650 battery, one of the most prevailing battery models in electric vehicles, caused by internal short circuit. An explosive load is applied to the 18650 battery FE model based on ABAQUS platform to simulate the internal short circuit. The FE model includes key components such as anode part, cathode part, multi-layered separator and the outside shell. Mechanical parameters are taken from previous studies [1] as well as current mechanical testing, with the consideration of temperature, strain rate and anisotropy effect. Result may provide future in-depth studies to study the lithium-ion battery explosion which are not available

from the real-world experiment such to guide the optimal design for safe battery manufacturing.

INTRODUCTION

Lithium-ion batteries (LIBs) are widely used in the modern industrial products, e.g. vehicle, robots, cellphones, aircrafts and among others. Due to inevitable wearing out or overstress characterized by various types of failure behavior of the anode, cathode, separator and casing, internal short circuits may be the prior causation for battery failure which may further cause thermal runaway, leading to fire or intensive explosion [2-4]. Thus increasing focus has been put on the explosive characteristic of the battery.

Previous pioneering work mainly focus on the experiments which have been conducted to study LIBs' thermal behavior after short circuit and thermal runaway. Doh et.al [5] studied the thermal and electrochemical behavior of C/LixCoO₂ cell during safety test such as overcharge, nail penetration and

impact tests. Kim et.al [6] studied the abnormal conditions (means the state of possible explosions with thermal runaway) through impact and heating tests and simulations. Jhu et al [7] employed a VSP2 (vent sizing package 2) adiabatic calorimeter to analyze the pressure and the temperature in thermal explosion hazards on 18650 cells. Ping et.al [8] used the deconvolution method to analyze the thermal behavior of lithium-ion battery at elevated temperature. Then Chen et.al [9] studied the thermal hazard features by calorimetric experimental trials under different SOCs (State of charges).

Some mechanical models [10-12] and electrochemical model [13] have been established under different conditions. For example, Sahraei et al [14, 15] established a FE model and detected the short circuit of the 18650 Li-ion cell under mechanical abuse condition with isotropic jelly roll model. However a numerical model used to explore the explosive behavior has not been yet discussed. In this paper, a FE model describing the explosion behavior of the battery cell is established based on the anisotropic model of 18650 cell with strain rate effect. To make it simple, a TNT equivalent quality is used to represent as the denotation of the explosion within the battery due to the internal short circuit. Explosion process and battery failure and disassembling behavior is then studied based on the suggested model.

METHOD

Constitutive model of the jellyroll

Our previous study [10, 16] revealed that the mechanical behavior of the battery cell are highly anisotropic, SOC dependent and strain rate dependent. Considering the fact that low SOC usually may hinder the battery explosion such that in this paper, SOC dependency is not considered and all explosions occur with high SOC value by assumption. During the elastic stage, engineering elastic constants are chosen for the anisotropic properties with the stress-strain constitutive law, which is shown as

$$\begin{Bmatrix} \varepsilon_{11} \\ \varepsilon_{22} \\ \varepsilon_{33} \\ \varepsilon_{12} \\ \varepsilon_{23} \\ \varepsilon_{31} \end{Bmatrix} = \begin{bmatrix} \frac{1}{E_{11}} & -\frac{\nu_{21}}{E_{22}} & -\frac{\nu_{31}}{E_{33}} & 0 & 0 & 0 \\ -\frac{\nu_{12}}{E_{11}} & \frac{1}{E_{22}} & -\frac{\nu_{32}}{E_{33}} & 0 & 0 & 0 \\ -\frac{\nu_{13}}{E_{11}} & -\frac{\nu_{23}}{E_{22}} & \frac{1}{E_{33}} & 0 & 0 & 0 \\ 0 & 0 & 0 & \frac{1}{G_{12}} & 0 & 0 \\ 0 & 0 & 0 & 0 & \frac{1}{G_{23}} & 0 \\ 0 & 0 & 0 & 0 & 0 & \frac{1}{G_{31}} \end{bmatrix} \begin{Bmatrix} \sigma_{11} \\ \sigma_{22} \\ \sigma_{33} \\ \sigma_{12} \\ \sigma_{23} \\ \sigma_{31} \end{Bmatrix} \quad (2)$$

where $\varepsilon_{ij} = \gamma_{ij} / 2$, $\sigma_{ij} = \tau_{ij} / 2$ ($i \neq j$), E_{ij} are the Young's modulus in x_i direction. G_{ij} is the shear modulus in direction j on the plane whose normal is in direction i , ν_{ij} is

the Poisson's ratio that corresponds to a contraction in direction j when an extension is applied in direction i . The parameters are calculated and determined in Ref. [10], which is $E_{11} = E_{22} = 500$ MPa, $E_{33} = 1500$ MPa, $G_{12} = 217$ MPa, $G_{23} = G_{31} = 300$ MPa, $\nu_{13} = \nu_{23} = 0.15$ and $\nu_{12} = 0.3$.

In plastic stage the Hill'48 anisotropic yield surface, with the hardening law $\sigma = A\varepsilon^n + B$ (where A and B are calculated as 930 MPa and 0.8 MPa respectively) chosen to model the jellyroll. The yield condition reads

$$\sigma_{Hill} = \sqrt{F(\sigma_2 - \sigma_3)^2 + G(\sigma_3 - \sigma_1)^2 + H(\sigma_1 - \sigma_2)^2 + 8L\sigma_{23}^2 + 8M\sigma_{31}^2 + 8N\sigma_{12}^2} \quad (3)$$

where σ_{Hill} is the Hill'48 equivalent stress, and the six constants F-N are measures of anisotropy, which can be obtained as follows

$$F = \frac{1}{2} \left(\frac{1}{R_{22}^2} + \frac{1}{R_{33}^2} - \frac{1}{R_{11}^2} \right) \quad (4)$$

$$G = \frac{1}{2} \left(\frac{1}{R_{33}^2} + \frac{1}{R_{11}^2} - \frac{1}{R_{22}^2} \right) \quad (5)$$

$$H = \frac{1}{2} \left(\frac{1}{R_{11}^2} + \frac{1}{R_{22}^2} - \frac{1}{R_{33}^2} \right) \quad (6)$$

$$L = \frac{3}{2R_{23}^2} \quad (7)$$

$$M = \frac{3}{2R_{13}^2} \quad (8)$$

$$N = \frac{3}{2R_{12}^2} \quad (9)$$

where R_{11} , R_{22} , R_{33} , R_{12} , R_{13} and R_{23} are the anisotropic yield stress ratios, which have been calculated in the previous study [10], which are 12.5, 1, 1, 12, 12, 17 respectively.

According to the previous study the rate dependent model can be further written as

$$\sigma = \begin{cases} (930\varepsilon^{3.4} + 0.8) & , \varepsilon \leq \varepsilon_c \\ [\sigma_c + 930(\varepsilon^{3.4} - \varepsilon_c^{3.4})]e^{0.02085\varepsilon^*} & , \varepsilon > \varepsilon_c \end{cases} \quad (10)$$

where $\varepsilon_c = 0.2$, and the units of the σ is MPa.

The strain failure criterion is chosen where the failure strain is set as $\varepsilon_f = 0.55$ measured by experiments and simulation.

Constitutive model of the shell

Mostly, the shell of 18650 LIB is made of steel or aluminum to maintain the shape of the jellyroll. The shell of the chosen battery (HP 602030 NCA-45 Ah/162 Wh) here is made of common steel with the mechanical properties obtained from Ref. [17]. Yong's modulus is $E_{shell} = 207$ GPa and Poisson's ratio is $\nu_{shell} = 0.3$. The strain hardening can be well represented by Johnson-Cook model [18] written as

$$\sigma = (0.6 + 600\bar{\varepsilon}^{p^n})(1 + 0.062\ln\bar{\varepsilon}^{p^*}) \quad (11)$$

where $\bar{\varepsilon}^p$ is plastic strain and $\dot{\bar{\varepsilon}}^{p*} = \frac{\dot{\varepsilon}^p}{\dot{\varepsilon}_0^p}$ is dimensionless plastic strain rate, with $\dot{\varepsilon}_0^p = 1 \text{ s}^{-1}$ as a reference strain rate. And the failure strain ε_f of the shell is about 0.04 from Ref. [19], and the units of the σ is GPa.

Modelling of the battery cell

A geometric model is established based on its real size as shown in Figure 1 which has key components such as anode part, cathode part, jellyroll and the outside shell whose thickness is 0.17, 0.17, 6.9 and 0.265 mm respectively. LIB has multi-layers of cathode, separator and anodes. Note that only one set of multi-layer is set up here to study its properties during explosion and others are regarded as jellyroll for simplicity. Separators are ignored in the explosive simulation for the temperature can raise up to 900°C [20] which is far beyond its melting point [21]. The specific size of the components and the element type are shown in Table 1 and a part of mechanical properties of cathode and anode are obtained from the nominal tensile stress-strain curves in Ref [1], and some other properties are obtained from Ref [10]

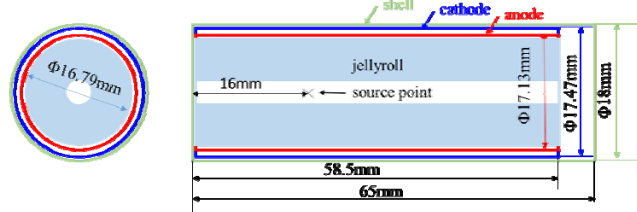


Figure 1 Schematic diagram of the LIB geometric model with dimensions

Table 1 the basic information of the components

Component	Element type	Mesh number
shell	S4R shell	17145
cathode	S4R shell	12753
anode	S4R shell	12519
jellyroll	C3D8R solid	1856

Modelling of the explosive load

An incident shock wave loading controlled by CONWEP model [22] is applied to the LIB FE model to simulate the explosive loading with similar strategies in Ref. [23]. LIB is considered as fluid-solid structure in the simulation because it has electrolyte between the cathode and anode. In consideration of the volatile of the electrolyte, the air is considered as medium in this simulation. In our case, the explosion is from the inner place while CONWEP is used to simulate the far-field air blast. To keep the minimum influence caused by the

multiple reflections of the pressure wave from the internal walls, we choose large quantity of TNT, i.e. 6 kg to produce the explosion. Thus CONWEP model is adopted where an explosion in air forms a highly compressed gas mass that interacts with the surrounding air, generating an outward-propagating shock wave. The resulting air blast wave is controlled by pressure-time curve as shown in Figure 2. For a given scaled distance, the maximum overpressure (above atmospheric), the arrival time, the positive phase duration, and the exponential decay coefficient for both the incident pressure and the reflected pressure are provided by the model which are defined by default value. Time of detonation is defined as time zero in the present simulation.

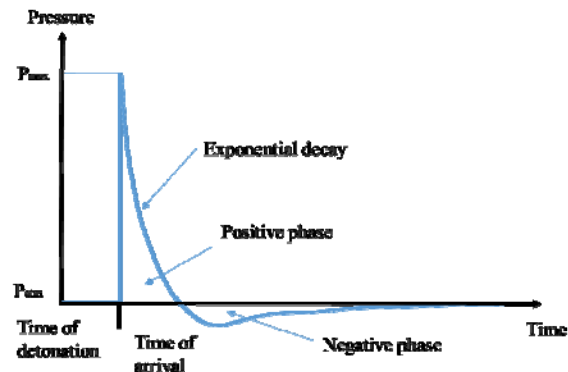


Figure 2 Pressure-time curve controlled by CONWEP model

The total pressure $P(t)$, on a surface due to the blast wave is a function of the incident pressure $P_{\text{incident}}(t)$, the reflected pressure $P_{\text{reflect}}(t)$, and the angle of incidence θ defined as the angle between the normal of the loading surface and the vector that points from the surface to the explosion source. The total pressure is defined as

$$P(t) = \begin{cases} P_{\text{incident}}(t)[1 + \cos \theta - 2 \cos^2 \theta] \\ + P_{\text{reflect}}(t) \cos^2 \theta; & \cos \theta \geq 0 \\ P_{\text{incident}}(t); & \cos \theta < 0 \end{cases} \quad (12)$$

A TNT equivalent quality is used to control the explosion energy. The source point of the finite element model is in the center line of the battery about 16 mm away from the negative pole shown in Figure 1 which is chose randomly, without loss of generality. Strain failure is adopted in this research and the failure strain of shell, cathode, anode and jellyroll is 0.04, 0.0066, 0.05 and 0.55 respectively [10, 24].

RESULTS

The morphology characteristics of the battery during the explosion under 6kg TNT equivalent quality is clearly depicted in the simulation as shown in Figure 3 (a) to (c) for cathode, anode and the battery shell respectively. The failure process of these components are similar: in the beginning of the explosion process, a crack appears along the axis direction of the battery, and a circular crack appears followed by. Then, more axial and circular cracks occur during the explosion, and some fragments are thrown around with certain velocities. The fragments of the

LIB explosion are lamellar which have good consistency with the experimental results gained from the Ref. [20] as shown in Figure 4.

The exploding times of the layers are different, i.e. the cathode layer is cracked firstly at $t=0.006$ s, then the initial crack appeared in the anode layer at $t=0.008$ s, then finally the battery shell is damaged at $t=0.01$ s although the incident shock wave arrives at the anode layer firstly, because the responsible reason should be the much smaller failure strain for the cathode than anode. And the fragments of these constituents differ obviously, e.g. the fragments of the cathode material is smaller than the shell and anode materials for its small failure strain.

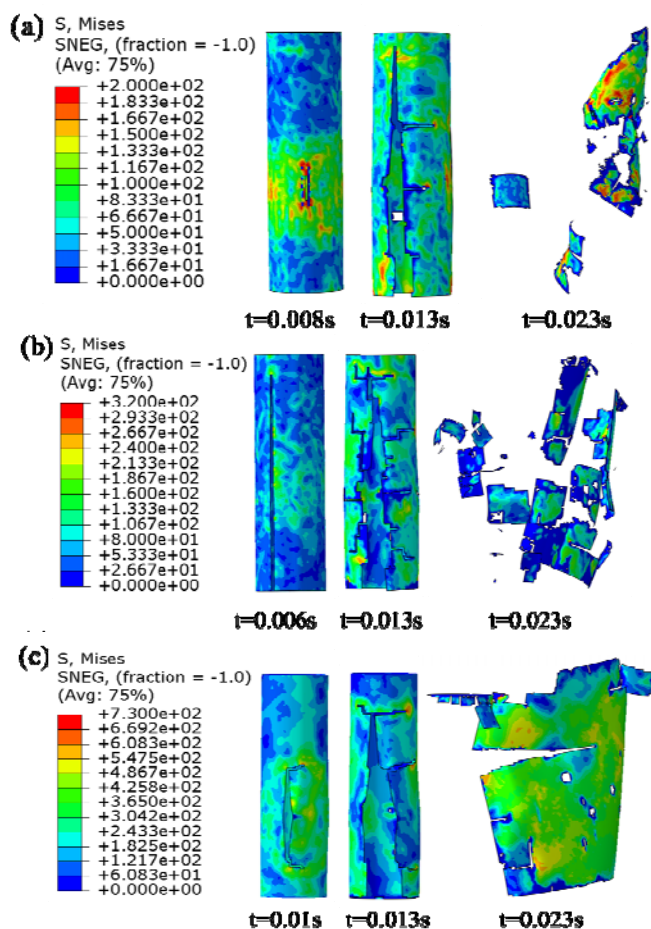


Figure 3 The morphology characteristics of the components evolution during the explosion time history: (a) cathode; (b) anode; (c) shell.

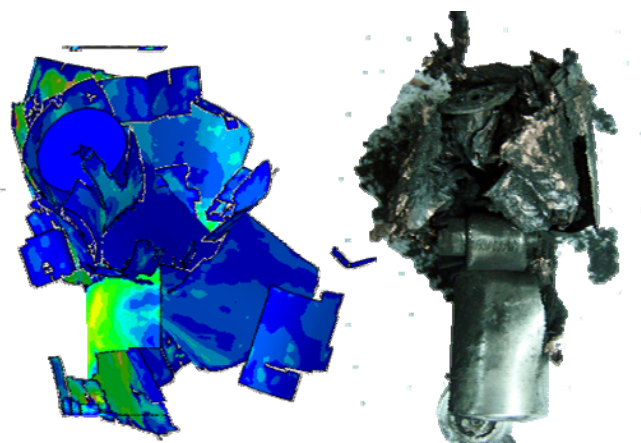


Figure 4 The comparison of the battery shell's morphology characteristics between simulation and experiment.

CONCLUDING REMARKS

Explosion behavior of lithium-ion battery is a great obstacle for the widespread of power battery but difficult to observe and quantitatively observed in a controlled manner in real-world experiment. This research discussed a method of modeling the lithium-ion battery explosion caused by internal short circuit based on the anisotropic and strain rate dependent finite element model of the same battery cell. The detailed failure process of the LIB during explosion was studied numerically and it was observed that the axial crack appeared at the beginning and followed by the circular crack. Different components of the battery may exhibit various failure behavior. The final morphology of the whole battery agreed well with the experiment test, verifying the model. Results may shed lights on the understanding of the battery explosion behaviors and guide the future safety design of lithium ion battery.

ACKNOWLEDGMENTS

This work is financially supported by the Fundamental Research Funds for the Central Universities, Beihang University, the startup fund for "Zhuoyue 100" titled professor, Beihang University, Opening fund of State Key Laboratory of Nonlinear Mechanics and Program for Zhejiang Leading Team of S&T Innovation (2011R50008-14).

REFERENCES

- [1] Lai, W.-J., Ali, M. Y., and Pan, J., 2014, "Mechanical behavior of representative volume elements of lithium-ion battery modules under various loading conditions," *Journal of Power Sources*, 248, pp. 789-808.
- [2] Zavalis, T. G., Behm, M., and Lindbergh, G., 2012, "Investigation of Short-Circuit Scenarios in a Lithium-Ion Battery Cell," *Journal of the Electrochemical Society*, 159(6), pp. A848-A859.
- [3] Ramadass, P., Fang, W., and Zhang, Z., 2014, "Study of internal short in a Li-ion cell I. Test method development using infra-red imaging technique," *Journal of Power Sources*, 248, pp. 769-776.

- [4] Fang, W., Ramadass, P., and Zhang, Z., 2014, "Study of internal short in a Li-ion cell-II. Numerical investigation using a 3D electrochemical-thermal model," *Journal of Power Sources*, 248, pp. 1090-1098.
- [5] Doh, C. H., Kim, D. H., Kim, H. S., Shin, H. M., Jeong, Y. D., Moon, S. I., Jin, B. S., Eom, S. W., Kim, H. S., Kim, K. W., Oh, D. H., and Veluchamy, A., 2008, "Thermal and electrochemical behaviour of C/LixCoO₂ cell during safety test," *Journal of Power Sources*, 175(2), pp. 881-885.
- [6] Kim, S., Lee, Y. S., Lee, H. S., and Jin, H. L., 2010, "A study on the behavior of a cylindrical type Li-Ion secondary battery under abnormal conditions," *Materialwissenschaft Und Werkstofftechnik*, 41(5), pp. 378-385.
- [7] Jhu, C. Y., Wang, Y. W., Shu, C. M., Chang, J. C., and Wu, H. C., 2011, "Thermal explosion hazards on 18650 lithium ion batteries with a VSP2 adiabatic calorimeter," *Journal of Hazardous Materials*, 192(1), pp. 99-107.
- [8] Ping, P., Wang, Q. S., Huang, P. F., Sun, J. H., and Chen, C. H., 2014, "Thermal behaviour analysis of lithium-ion battery at elevated temperature using deconvolution method," *Applied Energy*, 129, pp. 261-273.
- [9] Chen, W. C., Li, J. D., Shu, C. M., and Wang, Y. W., 2015, "Effects of thermal hazard on 18650 lithium-ion battery under different states of charge," *J. Therm. Anal. Calorim.*, 121(1), pp. 525-531.
- [10] Xu, J., Liu, B., Wang, X., and Hu, D., 2015(submitted), "Mechanical Model of 18650 Lithium-ion Battery with Coupled Strain Rate and SOC Dependencies," *Journal of Power Sources*.
- [11] Prueter, P. E., "Using explicit finite element analysis to simulate the dynamic response and predict the structural damage associated with a real-life process equipment failure due to an internal detonation," Proc. Process Safety Spotlights 2014 - Topical Conference at the 2014 AIChE Spring Meeting and 10th Global Congress on Process Safety, pp. 173-186.
- [12] Pannala, S., Turner, J. A., Allu, S., Elwasif, W. R., Kalnaus, S., Simunovic, S., Kumar, A., Billings, J. J., Wang, H., and Nanda, J., 2015, "Multiscale modeling and characterization for performance and safety of lithium-ion batteries," *J. Appl. Phys.*, 118(7), p. 14.
- [13] Chiu, K.-C., Lin, C.-H., Yeh, S.-F., Lin, Y.-H., and Chen, K.-C., 2014, "An electrochemical modeling of lithium-ion battery nail penetration," *Journal of Power Sources*, 251, pp. 254-263.
- [14] Sahraei, E., Campbell, J., and Wierzbicki, T., 2012, "Modeling and short circuit detection of 18650 Li-ion cells under mechanical abuse conditions," *Journal of Power Sources*, 220, pp. 360-372.
- [15] Wierzbicki, T., and Sahraei, E., 2013, "Homogenized mechanical properties for the jellyroll of cylindrical Lithium-ion cells," *Journal of Power Sources*, 241, pp. 467-476.
- [16] Xu, J., Liu, B., and Hu, D., 2016(in press), "State of Charge Dependent Mechanical Integrity Behavior of 18650 Lithium-ion Batteries," *Scientific Reports*. (In press)
- [17] Greve, L., and Fehrenbach, C., 2012, "Mechanical testing and macro-mechanical finite element simulation of the deformation, fracture, and short circuit initiation of cylindrical Lithium ion battery cells," *Journal of Power Sources*, 214, pp. 377-385.
- [18] Xu, J., Liu, B., Wang, L., and Shang, S., 2015, "Dynamic mechanical integrity of cylindrical lithium-ion battery cell upon crushing," *Eng. Fail. Anal.*, 53, pp. 97-110.
- [19] Zhang, X., and Wierzbicki, T., 2015, "Characterization of plasticity and fracture of shell casing of lithium-ion cylindrical battery," *Journal of Power Sources*, 280, pp. 47-56.
- [20] Jhu, C.-Y., Wang, Y.-W., Shu, C.-M., Chang, J.-C., and Wu, H.-C., 2011, "Thermal explosion hazards on 18650 lithium ion batteries with a VSP2 adiabatic calorimeter," *Journal of Hazardous Materials*, 192(1), pp. 99-107.
- [21] Xu, J., Wang, L., Guan, J., and Yin, S., "Coupled effect of strain rate and solvent on dynamic mechanical behaviors of separators in lithium ion batteries," *Mater. Des.* (In press)
- [22] Hibbitt, Karlsson, and Sorensen, 2001, ABAQUS/standard user's Manual, Hibbitt, Karlsson & Sorensen.
- [23] Park, J., and Choi, H.-J., 2015, "Experiments and numerical analyses of HB400 and aluminum foam sandwich structure under landmine explosion," *Composite Structures*, 134, pp. 726-739.
- [24] Sahraei, E., Kahn, M., Meier, J., and Wierzbicki, T., 2015, "Modelling of cracks developed in lithium-ion cells under mechanical loading," *Rsc Advances*, 5(98), pp. 80369-80380.